Phase Dynamics at Microtubule Ends: The Coexistence of Microtubule Length Changes and Treadmilling

Kevin W. Farrell, Mary Ann Jordan, Herbert P. Miller, and Leslie Wilson

Department of Biological Sciences, University of California, Santa Barbara, California 93106

Abstract. The length dynamics both of microtubule-associated protein (MAP)-rich and MAP-depleted bovine brain microtubules were examined at polymer mass steady state. In both preparations, the microtubules exhibited length redistributions shortly after polymer mass steady state was attained. With time, however, both populations relaxed to a state in which no further changes in length distributions could be detected. Shearing the microtubules or diluting the microtubule suspensions transiently increased the extent to which microtubule length redistributions occurred, but again the microtubules relaxed to a state in which changes in the polymer length distributions were not detected. Under steady-state conditions of constant polymer mass and stable microtubule length distribution, both MAP-rich and MAP-depleted microtubules exhibited behavior consistent with treadmilling. MAPs strongly suppressed the magnitude of length redistributions and the steady-state treadmilling rates. These data indicate that the inherent tendency of microtubules in vitro is to relax to a steady state in which net changes in the microtubule length distributions are zero. If the basis of the observed length redistributions is the spontaneous loss and regain of GTP-tubulin ("GTP caps") at microtubule ends, then in order to account for stable length distributions the microtubule ends must reside in the capped state far longer than in the uncapped state, and uncapped microtubule ends must be rapidly recapped. The data suggest that microtubules in cells may have an inherent tendency to remain in the polymerized state, and that microtubule disassembly must be induced actively.

ALTHOUGH it is known that microtubules are involved in many cell functions (9, 32), in most cases it is not clear how microtubules perform these functions or how their activities in cells are regulated. One approach to these questions has been the study of microtubule polymerization in vitro, while a second approach, made possible by the recent development of appropriate molecular probes, has been the study of microtubule dynamics in cells (reviewed in reference 24).

Microtubules were initially viewed as polymers in simple equilibrium with a fixed (critical) concentration of tubulin subunits (14, 20, 21, 31), a view largely consistent with the behavior of labile microtubules in cells (17, 18, 35). Evidence that this view was overly simple was initially obtained by Margolis and Wilson (27), who used radiolabeled GTP as a probe for tubulin addition and loss at the ends of a microtubule-associated protein (MAP)[1]-rich bovine brain microtubule protein preparation in vitro. They found that in the presence of GTP and a GTP-regenerating system, these microtubules were not at true equilibrium, but were at steady state. They interpreted their data as indicating that net addition of tubulin subunits at one microtubule end was exactly balanced by the net loss of subunits from the opposite end; a behavior called "treadmilling" or "flux". Evidence consistent with treadmilling in vitro was subsequently obtained for other microtubule preparations (2, 8, 10, 33), and has included direct observation by electron microscopy (33).

The concept of subunit flux was initially described by Wegner for actin filaments (36). Wegner recognized that the hydrolysis of ATP during actin polymerization could result in the establishment of different critical concentrations for growth at the two ends of the filaments, and thus result in the net addition of actin at one filament end and loss of actin at the opposite end. For microtubules, the energy source is GTP hydrolysis rather than ATP hydrolysis.

However, it is clear that GTP hydrolysis at microtubule ends could be used to create other kinds of assembly behaviors (24). A different kind of dynamic behavior of microtubules in vitro that is also thought to involve GTP hydrolysis was recently described by Mitchison and Kirschner (29, 30) and by Kristofferson et al. (25). These investigators have observed that the mean length of MAP-depleted brain microtubules increased while the number of microtubules in suspension decreased with time, even though the microtubule polymer mass remained constant. This behavior has been termed "dynamic instability". These investigators have suggested that dynamic instability is due to transitions between

1. *Abbreviations used in this paper*: MAP(s), microtubule-associated protein(s).

two phases at microtubule ends (5, 6, 7, 15, 24, 30). In one phase, microtubule ends are relatively stable and elongate slowly, while in the second phase, microtubule ends are extremely unstable and the microtubules depolymerize cataclysmically. Because the numbers of microtubules were observed to decrease continuously at polymer mass steady state, it was proposed that transitions between the two phases occur very infrequently (25, 30).

The mechanistic basis for the putative phase transitions is not known, but the gain and loss of regions of GTP-tubulin at the ends of microtubules has been proposed as a reasonable possibility (see 24). The dynamic instability model views microtubules as being inherently unstable. Mitchison and Kirschner have further proposed that selective stabilization of unstable microtubules is an important aspect of microtubule-mediated cell shape determination and spindle morphogenesis (24).

Certain aspects of the dynamic instability model are incompatible with data obtained previously in vitro, both with MAP-rich and MAP-depleted microtubule populations, which indicated that microtubules at polymer mass steady state attain stable length distributions (8, 39). In the present report, we have investigated how microtubules could exhibit such apparently incompatible behaviors as treadmilling and dynamic instability, using both MAP-rich and MAP-depleted microtubule preparations at polymer mass steady state. The data demonstrate that both microtubule preparations exhibit length redistributions transiently after reaching polymer mass steady state and then relax to a state in which further changes in the length distributions are not detectable. Under these conditions treadmilling behavior is observed. Further dynamic instability behavior can be induced by shearing or by dilution, but the perturbed microtubule suspensions relax to a state in which further changes in the length distributions are not detectable. The MAPs strongly suppress both dynamic instability and treadmilling behaviors quantitatively, but do not change the observed behavior qualitatively. Our data indicate that rather than being inherently unstable, microtubule polymers in vitro are inherently stable.

Materials and Methods

Preparation of MAP-rich Bovine Brain Microtubules

Bovine brain microtubule protein consisting of 80 ± 1% tubulin and 20 ± 1% MAPs as determined by SDS PAGE, Coomassie staining, and laser densitometry (Ultroscan XL; LKB Produkter AB, Sweden) was isolated without glycerol by modification (13) of the procedure of Asnes and Wilson (1) and stored frozen as microtubule pellets at −70°C. For reassembly, pellets were resuspended by Dounce homogenization in 100 mM 2-(*N*-morpholino) ethane sulfonic acid (MES), 1 mM EGTA, and 1 mM $MgSO_4$, pH 6.8 (MEM buffer), and after a 15-min incubation at 0°C, solutions were centrifuged (29,900 *g*, 10 min, 4°C, SS-34 rotor, Sorvall RC5). To assemble MAP-rich microtubules, GTP (0.1–0.2 mM) and a GTP-regenerating system consisting of 10 mM acetyl phosphate and 0.1 IU/ml acetate kinase (26) were added and the temperature raised to 30°C.

Preparation of MAP-depleted Bovine Brain Microtubules

The preparation of MAP-depleted tubulin solutions and the assembly of microtubules from them were performed essentially as described by Mitchison and Kirschner (29). Pellets of three-cycle bovine brain MAP-rich microtubules (see above) were resuspended by Dounce homogenization in column buffer (50 mM Pipes, 1 mM EGTA, 0.2 mM $MgSO_4$, pH 6.8) plus 0.1 mM GTP. After a 20-min incubation at 0°C the solution was centrifuged (150,000 *g*, 30 min, 4°C). The supernatant (50–60 mg total protein) was applied to a 30-ml phosphocellulose column (P11; Whatman Chemical Separation, Ltd., England) equilibrated in column buffer at 4°C. Peak flow-through fractions were pooled, GTP was added (0.1 mM), and the tubulin was frozen in aliquots in liquid nitrogen and stored at −70°C. This preparation consisted of 98.5 ± 1.3% tubulin (method described above). Immediately before assembly, tubulin was thawed, clarified by centrifugation (29,900 *g*, 20 min, 4°C), and the supernatant concentrated to 3–6 mg/ml by centrifugation using a Centricon 30 (Amicon Corporation, Danvers, MA). To prepare microtubule seeds, MAP-depleted tubulin (3–6 mg/ml) was dialyzed overnight (4°C) against a 200-fold excess of Pipes polymerization buffer (80 mM Pipes, 0.8 mM $MgSO_4$, 1 mM EGTA, 0.1 mM GTP, and regenerating system) plus 30% glycerol, then assembled at 37°C with or without shearing (three to four passes, 0.5-in. 25-gauge needle). Microtubule assembly was initiated by diluting seeds 1/50–1/100 into MAP-depleted tubulin (36–55 μM) in Pipes polymerization buffer at 37°C.

Preparation of Microtubules Differentially Labeled with [^{3}H] and [^{14}C]Guanine Nucleotides

Determination of Dynamics of Tubulin Exchange with Steady-state Microtubules. To determine simultaneously the rate of tubulin gain and loss at opposite microtubule ends at steady state, we used a pulse-chase double label procedure with [^{3}H]- and [^{14}C]guanine nucleotide (11, 22). Microtubules were initially labeled throughout their lengths with [^{14}C]guanine nucleotide by polymerizing them to steady state without shearing in the presence of [^{14}C]GTP (0.1–0.2 mM, 6–11 Ci/mol final specific activity), i.e., both ends become labeled with ^{14}C-nucleotide. Under the conditions used, the stoichiometry of [^{14}C]guanine nucleotide per mole of tubulin dimer in microtubules ranged from 0.3–0.8. At least 20 min after polymer mass steady state had been reached as determined by turbidimetry, a trace quantity of [^{3}H]GTP was added to the ^{14}C-labeled microtubules to initiate the [^{3}H]guanine nucleotide pulse to determine burst uptake and assembly end uptake (38–137 Ci/mol final specific activity; final GTP concentration was altered negligibly; time of pulse was 50 min postinitiation for MAP-rich preparations, 66 min postinitiation for MAP-depleted preparations). Excess (25-fold) unlabeled GTP was added 28–60 min after initiation of the [^{3}H]GTP pulse to serve as a chase for both isotopes in order to determine burst loss and disassembly end tubulin loss. MAP-rich microtubules were collected on glass-fiber filters (37) and MAP-depleted microtubules were collected by sedimentation (reference 5, see below) for analysis of radiolabel incorporation.

Steady-state rates of tubulin incorporation at assembly ends were calculated from least squares linear regressions of the rates of [^{3}H]GTP uptake into microtubules from 8 to 40 min after radioisotope addition to MAP-rich microtubules and from 7 to 27 min after addition to MAP-depleted microtubules. Rates of tubulin loss at steady-state disassembly ends were calculated similarly from the rates of [^{14}C]GTP loss from MAP-rich microtubules between 8 and 50 min and from MAP-depleted microtubules between 5.5 and 58 min after initiation of the chase with excess unlabeled GTP.

Determination of Rate and Extent of Tubulin Subunit Readdition to Microtubules after Dilution. MAP-rich microtubule protein (5.17 mg/ml, with a critical concentration of 0.44 mg/ml determined by sedimentation [150,000 *g*, 45 min, 30°C]), was polymerized to steady state at 30°C in MEM buffer plus GTP-regenerating system and [^{14}C]GTP (0.2 mM GTP, specific activity, 8.4 Ci/mol) to label the microtubules uniformly with [^{14}C]GTP for determination of the stoichiometry (0.58) of GTP/tubulin incorporation. Microtubules were sheared (six passes through a 1.5-in. 22-gauge needle) 32 min after initiation of assembly, i.e., after attainment of turbidimetric steady state. 90 min after initiation, 1 vol of microtubule suspension was added to 3 vol of MEM buffer (30°C) containing the same concentration and specific activity [^{14}C]GTP, regenerating system, and a trace of [^{3}H]-GTP (107 Ci/mol). After gently pipetting up and down twice with a Pasteur pipette to mix (0.9 min), the mixture was sampled at timed intervals to determine microtubule lengths by electron microscopy and radiolabel incorporation by glass-fiber filter assay. The critical concentration of the diluted suspension was 0.32 mg/ml total microtubule protein.

Sedimentation Assay for Determination of Tubulin Exchange Dynamics with Steady-state MAP-depleted Microtubules. MAP-depleted microtubules were assembled at 37°C in the presence of [^{14}C]GTP (described above). After 10–15 min but before attainment of polymer mass steady state, aliquots (75 μl) of the suspension were gently transferred to a series of airfuge tubes in a 37°C water bath using cut-off Pipetman tips to minimize shearing. After at least 1 h of polymerization, 7.5 μl of [^{3}H]GTP solution was added to each tube with a gentle upward spiral motion of the pipette

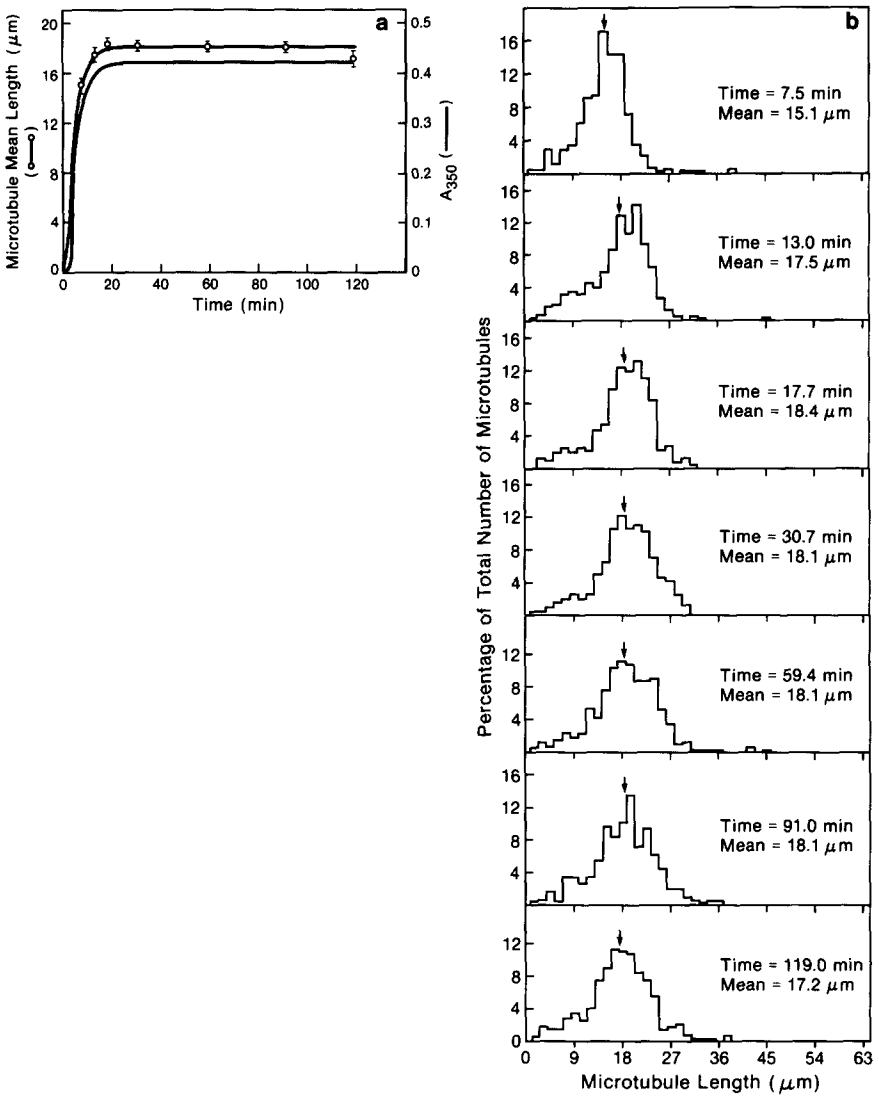

Figure 1. The length dynamics of MAP-rich microtubules at polymer mass steady state. Bovine brain microtubules were assembled undisturbed to steady state at 30°C from a MAP-rich tubulin solution (total protein concentration 2.2 mg/ml) in MEM buffer containing 0.1 mM GTP and a GTP-regenerating system. (*a*) Microtubule assembly was followed turbidimetrically by absorbance at 350 nm (*solid line*). The lengths of the microtubules were measured after fixation in MEM-buffered glutaraldehyde, from electron micrograph prints at a final magnification of 2,800×. At least 335 microtubules were measured per time point. (*Open circles*) Mean microtubule length. (*b*) Distribution of microtubule lengths. Arrows indicate the means. Error bars indicate ±1 SEM. The number concentration of microtubules in solution was 5.1×10^{-10} M.

tip and no further mixing. At each pulse or chase time point, triplicate sample tubes were centrifuged in an airfuge (29 psi, 37°C, 2 min; Beckman Instruments, Inc., Palo Alto, CA) after which the airfuge was allowed to come to a stop. Supernatants were aspirated, and pellets were cleaned with three overlayerings of 0.1-M Pipes buffer containing 30% glycerol and 10% dimethyl sulfoxide. Tubes containing cleaned pellets were added to 10 ml Fluorosol (National Diagnostics, Somerville, NJ) for determination of incorporated radioactivity. Background was determined by adding radiolabeled GTP to unlabeled microtubule suspensions simultaneously with an excess of unlabeled GTP (2.7 mM), centrifuging immediately, and processing as described above.

Microtubule Length Determinations. Microtubules (5–10 μl) were fixed by slow injection into 0.2–1% glutaraldehyde in polymerization buffer (30 or 37°C) through cut-off Pipetman tips using a circling and rising motion, followed by gentle mixing. Fixed microtubules were diluted further into buffered glutaraldehyde to obtain optimal densities of microtubules on the grids (final protein concentration, 20 μg/ml for MAP-containing microtubules and 3 μg/ml for MAP-free microtubules, which are generally longer in length). Within 20 min a drop of fixed microtubules was placed on a parlodion- and carbon-coated grid of 75–200 mesh. After 30 s it was incompletely wicked off (to avoid mechanical stress), replaced with one drop aqueous cytochrome C (1 mg/ml) followed by three drops distilled water (incompletely wicked off), then one drop 1% aqueous uranyl acetate (20 s; wicked off).

Fields of microtubules were selected solely on the basis of containing an appropriate density of microtubules for measurement and were photographed at magnifications ranging from 230× (for MAP-free) to 4400× (for MAP-containing) with a Philips EM300 electron microscope (60 or 80 kV) calibrated daily at the magnifications used. Negatives were printed at two and a half times enlargement and the lengths of all microtubules contained entirely in a field were measured with a Zeiss MOP-3 digitizer by a person who was unaware of the sample identity.

Protein Assay

Protein was determined by the method of Bradford (3) using bovine serum albumin as the standard.

Reagents

MES, Pipes, EGTA, GTP (types I and II), acetate kinase (EC 2.7.2.1), acetyl phosphate, and Coomassie Blue R were obtained from Sigma Chemical Co., St. Louis, MO. [^{3}H]GTP was obtained from ICN, Irvine, CA, and [^{14}C]GTP was obtained from Research Products International Corp., Mt. Prospect, IL. Glutaraldehyde (25%, electron microscope grade) was obtained from Ted Pella, Inc., Tustin, CA. All other chemicals were reagent grade.

Results

Length Dynamics of MAP-rich Microtubules

The steady-state dynamics of MAP-rich microtubules were examined under three types of experimental conditions: unperturbed, sheared, and diluted. For the unperturbed condi-

Table I. Change in Mean Length of an Unsheared and Undisturbed MAP-rich Microtubule Population with Time at Steady State

Time at steady state	Microtubule mean length	No. of microtubules measured
min	*μm*	
0	5.2	428
22	6.1	418
42	6.6	413
43	6.5	430
58	6.8	424
95	7.0	389
120	6.9	463
156	7.2	414
157	7.1	388

Small changes in the mean length of unsheared and undisturbed MAP-rich microtubule populations were observed occasionally. MAP-rich microtubule protein (4.5 mg/ml) was polymerized to steady state (30 min, determined by turbidity) without shearing. Samples were fixed at the designated times and lengths were measured (final print magnification, 2,800×). The mean length increased for nearly 1 h after attaining steady state, after which it stabilized. The length distributions (not shown) were Poisson-like at 0 and 22 min after steady state, with large numbers of microtubules <4 μm in length. By 1 h they had become nearly normally distributed about the mean. Standard error of the mean was ±0.1 μm.

tion, MAP-rich microtubules were assembled at 30°C without disturbing the microtubules, either before steady state or after steady state had been reached. Assembly was monitored turbidimetrically and samples were taken for length determinations before steady state and for 100 min after attainment of steady state. Under these conditions net redistribution of microtubule lengths either did not occur, or the extent of redistribution was very small once polymer mass steady state had been reached. In the experiment shown in Fig. 1, neither the shape of the length distribution nor the mean length varied detectably at steady state. This result has been observed repeatedly. In a few experiments, however, small increases in the mean length were observed at polymer mass steady state (Table I). However, in every case the length redistribution was small, and the length distribution stabilized within 60 min of reaching steady state.

The second type of experimental condition examined involved shearing the microtubules. In the experiment shown in Fig. 2, a microtubule suspension was sheared 6–7 min after initiation of assembly, shortly before reaching polymer mass steady state (10 min). In contrast to the results of the experiment shown in Fig. 1, the mean length continued to increase after the polymer mass had reached plateau (1 μm increase 37 min after attainment of steady state). Concomitantly the length distribution broadened and became more normally distributed about the mean. Thereafter, no further change was detected in either length distribution or mean length (Fig. 2 *b*). When microtubules were sheared at steady state after the length distribution had stabilized, a small redistribution of lengths was induced (Fig. 3). Before shearing, the steady-state mean length was stable at 5.0 ± 0.1 μm. Immediately after shearing, the mean length decreased to 2.3 ± 0.1 μm but increased by 0.9 μm during the next 30 min, then remained constant for the next 120 min.

The results shown in Figs. 2 and 3 are typical of MAP-rich microtubule preparations. Although we repeatedly observed that shearing enhanced steady-state length redistributions,

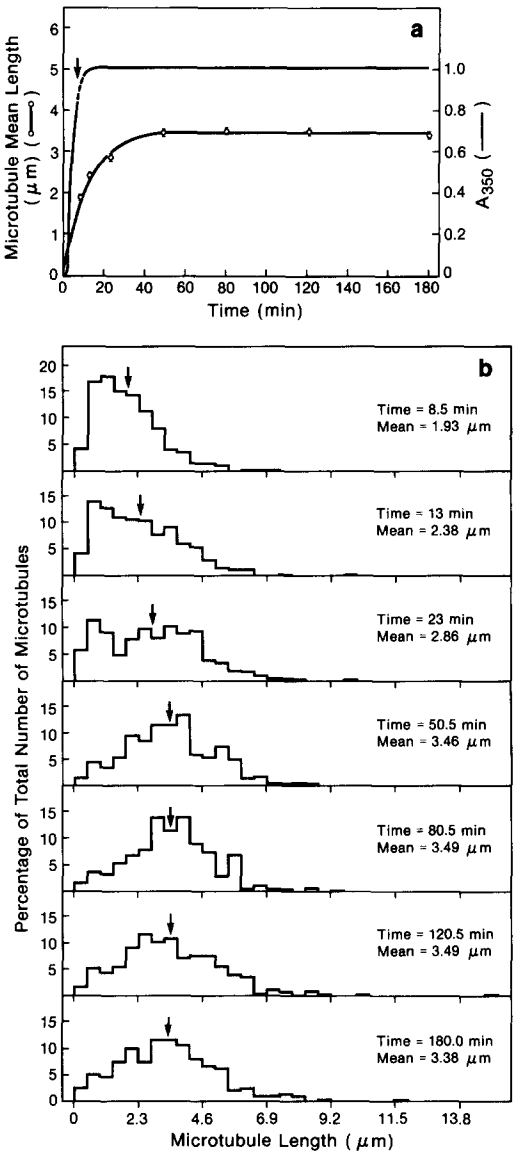

Figure 2. Shearing MAP-rich microtubules before the attainment of steady state. (*a*) Microtubules were assembled from MAP-rich tubulin solutions (total protein concentration, 6.5 mg/ml) as described in Fig. 1, except that the microtubules were sheared (*arrow*) before steady state. Assembly was monitored turbidimetrically at 350 nm (*solid line*) and the microtubule lengths (*open circles*) were determined after fixation in MEM-buffered glutaraldehyde (final print magnification of 6,500–11,000×, >400 microtubules per time point. (*b*) Microtubule length distributions at the time points given in *a*. Arrows indicate mean length of the microtubules. Error bars indicate ±1 SEM. The number concentration of microtubules in solution was 6.0 × 10^{-9} M.

the length redistributions and the mean length increases were invariably small and were at least an order of magnitude smaller than the changes in sheared MAP-depleted microtubule preparations seen by Mitchison and Kirschner (30).

Changes in the mean length of microtubules also occurred with the third type of experimental treatment in which steady-state MAP-rich microtubules were diluted fourfold into warm reassembly buffer (Fig. 4). The mean length of the microtubule population immediately before dilution was stable at 3.3 ± 0.1 μm. After dilution the mean length initially

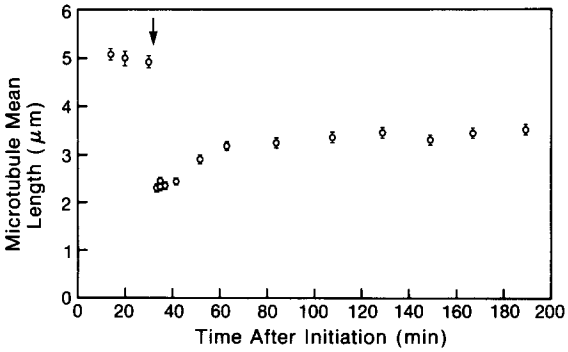

Figure 3. Shearing MAP-rich microtubules at steady state. Microtubules were assembled from MAP-rich microtubule protein solutions (5.2 mg/ml) as described in Fig. 1. Microtubule lengths were determined after fixation in MEM-buffered glutaraldehyde (final magnification of 6,500×, >400 microtubules per time point). The arrow indicates the time of shearing. Error bars indicate ±1 SEM.

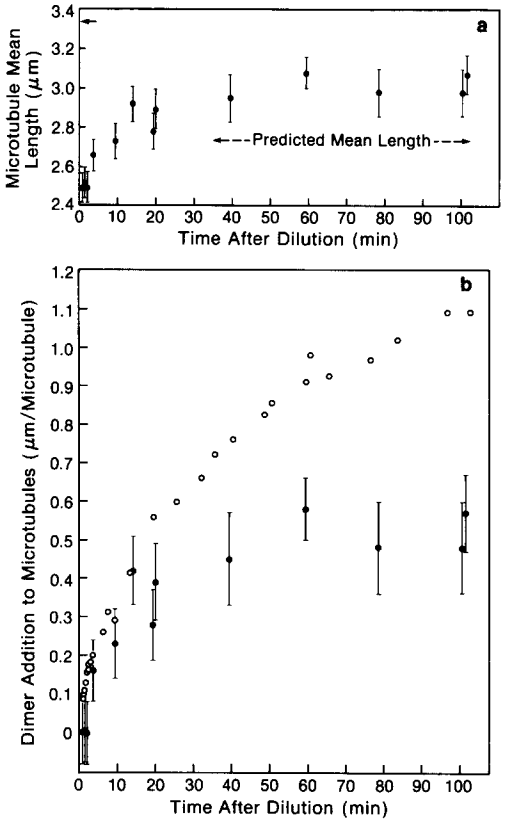

Figure 4. Effect of dilution on microtubule length distributions of MAP-rich microtubules. MAP-rich microtubules at polymer mass steady state (total protein concentration before dilution 5.17 mg/ml) were diluted fourfold into MEM (30°C) containing 0.1 mM [^{3}H]GTP (107 Ci/mole). Microtubule lengths were determined after fixation (final print magnification, 6,500×, >400 microtubules measured per time point). (*a*) Microtubule mean length before dilution (*arrow*) and for 100 min after dilution. Error bars indicate ±1 SEM. The predicted mean length of the microtubules was calculated from the dilution factor (fourfold), the microtubule critical concentration (0.44 and 0.32 mg/ml before and after dilution, respectively), and the microtubule length distribution immediately before dilution, assuming a simple homogeneous microtubule–tubulin equilibrium. (*b*) Dimer addition to the microtubules was calculated from the increase in the mean length of the microtubules shown in *a* (*solid circles*) and from the amount of radiolabeled guanine nucleotide incorporated into the microtubules (*open circles*).

decreased to 2.5 ± 0.1 μm and then increased to 3.0 ± 0.1 μm during the next 60 min, after which time no further change in either the mean length (Fig. 4) or length distribution (not shown) occurred. The mean length of 2.5 μm observed immediately after dilution and the 3.0 μm mean length observed finally are different from the expected mean length of 2.8 μm calculated from the length distribution before dilution and the dilution factor, assuming a simple Oosawa (31) equilibrium. These results have been observed repeatedly, but with some variation in the amount of mean length increase.

Tubulin subunit exchange with microtubules was measured simultaneously in the foregoing experiment by including [^{3}H]GTP in the dilution buffer. Uptake of radiolabel into the microtubules occurred immediately after dilution and continued approximately linearly with time after the microtubule length distribution had stabilized (Fig. 4 *b*). The net addition of tubulin subunits to microtubules during the dilution-induced length redistribution was calculated from the radiolabel incorporated into the microtubules, and, independently, from the increase in mean length of the microtubule population. The two estimates agreed closely during the initial period after dilution, during which time most (~70%) of the mean length increase occurred (Fig. 4 *b*, first 15 min after dilution). The data are consistent with the interpretation that some subunits lost from microtubules by depolymerization subsequently regrew onto surviving microtubules to contribute to the mean length increase. The subsequent uptake of radiolabel after the length distribution stabilized is consistent with treadmilling (38, 39).

Length Dynamics of MAP-depleted Microtubules at Steady State

The rapid and extensive length redistributions reported by Mitchison and Kirschner (30) were observed using MAP-depleted microtubule preparations that had been sheared. We therefore examined whether and to what extent shearing enhanced length redistributions in MAP-depleted microtubule populations and whether length redistributions occurred in unperturbed populations.

Polymerization in two identical MAP-depleted tubulin solutions was initiated by addition of preformed microtubule "seeds." One sample was undisturbed, while a second sample was sheared before reaching polymer mass steady state (Materials and Methods). In the unperturbed suspension, both the mean length of the microtubules (Fig. 5 *a*) and the length distribution (Fig. 5 *b*) remained essentially constant throughout steady state. In contrast, shearing the microtubules induced rapid and extensive length redistributions. Soon after reaching polymer mass steady state the mean length of the sheared microtubules was 32.8 μm (Fig. 5 *a*, time, 51 min). The mean length increased to 69 μm during the following 63 min. The sheared microtubule lengths initially exhibited a Poisson-like distribution. However, with time at steady state, the fraction of shorter microtubules in the population decreased and the fraction of longer microtu-

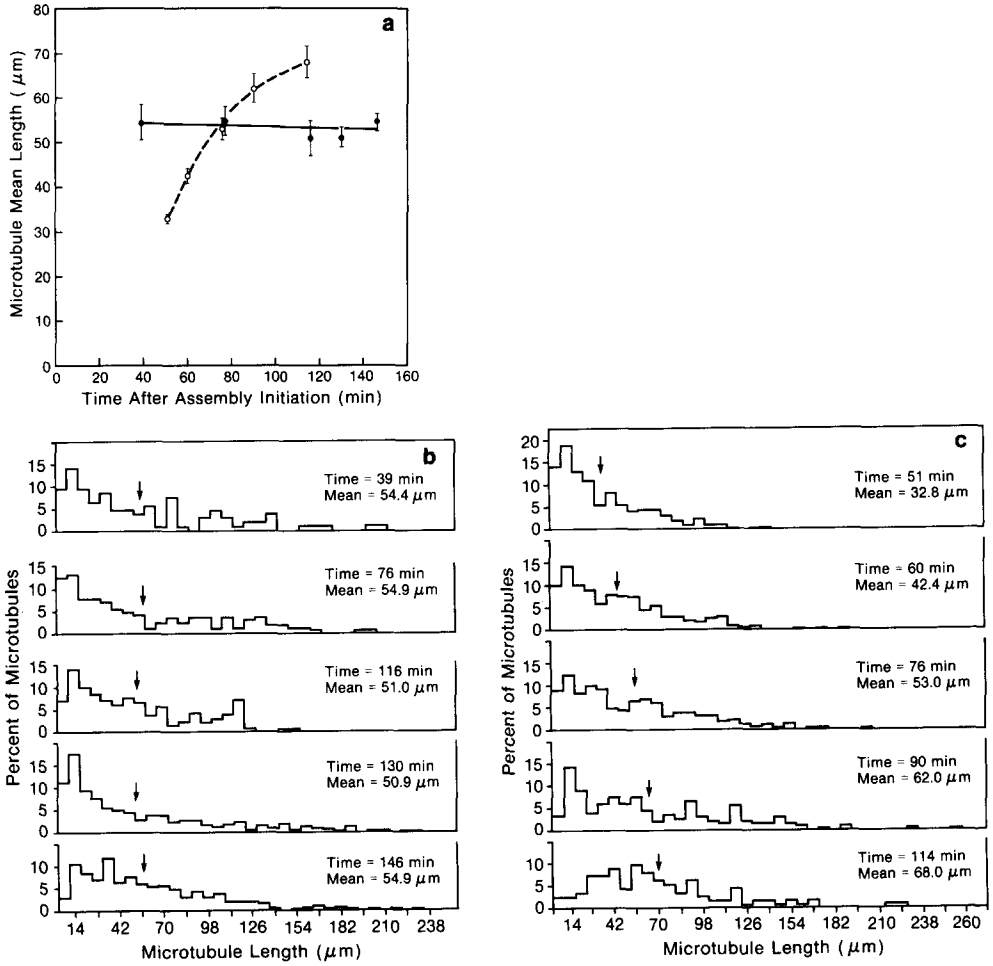

Figure 5. Effect of shearing on lengths of MAP-depleted microtubules. Microtubules were assembled to steady state (35 min) from MAP-depleted tubulin solutions (4.8 mg/ml) in Pipes polymerization buffer. The unsheared sample was seeded (76 μl seeds in 3.8 ml tubulin) and allowed to polymerize undisturbed. The second sample was seeded (12 μl in 3.8 ml tubulin) and sheared at 21 min. Since shearing the microtubules induced some depolymerization, the sheared microtubules were allowed to reestablish polymer mass steady state for 30 min before aliquots were removed for length measurements. The lengths were determined after fixation (final print magnification, 570×, >100 microtubules measured per time point). (*a*) Mean lengths of sheared (*open circles*) and unsheared (*solid circles*) samples. Error bars indicate ±1 SEM. Distributions are shown in *b* for the unsheared sample and *c* for the sheared sample. Arrows indicate mean length of the microtubule distributions.

bules increased, resulting in a spreading of the distribution towards longer microtubules (Fig. 5 *c*).

The observation that the mean length of the sheared microtubule sample increased beyond that of the unsheared sample (Fig. 5 *a*) suggests that the length distribution stability of the unsheared sample is not an artifact resulting from an inability to measure longer microtubules. Neither does the stability of the unsheared sample seem to be generated artifactually by breakage of longer microtubules, because no increase in the fraction of shorter microtubules was observed (Fig. 5 *b*). With unperturbed MAP-depleted microtubule preparations, a relatively small increase in mean length was observed in some experiments (e.g., Table II), but distributions always stabilized within 60 min at steady state.

Table II. Change in Mean Length of an Unsheared and Undisturbed MAP-depleted Microtubule Preparation with Time at Polymer Mass Steady State

Time at steady state	Microtubule mean length	SEM	No. of microtubules measured
min	*μm*	*μm*	
0	54.6	1.9	229
14	59.8	2.3	236
28	60.0	2.2	260
38	59.7	2.5	218
55	59.0	2.1	327
78	61.8	2.0	345

MAP-depleted microtubule protein (2.7 mg ml^{-1}) was polymerized to steady state (31 min, determined by turbidimetry) without shearing. Samples were fixed at the designated times and their lengths measured (final print magnification, 760×). The mean length increased by 5 μm during the 14 min after attainment of steady state, after which it stabilized.

The Dynamics of Tubulin Exchange when Microtubule Length Distributions Are Stable

We performed double-label pulse-chase experiments with MAP-rich and MAP-depleted microtubules to examine the dynamics of tubulin exchange at microtubule ends when length distributions were stable (see Materials and Methods). MAP-rich or MAP-depleted tubulin solutions were assembled to steady state in the presence of [^{14}C]GTP. At steady state, a pulse (trace) of [^{3}H]GTP was added, and after an additional 60 min of incubation, a 25-fold excess of unlabeled GTP was added.

The results of one such experiment for MAP-rich microtubules is shown in Fig. 6. During the pulse, there was an initial rapid burst of [^{3}H]GTP incorporation into microtubules, followed by a slower phase during which label uptake proceeded approximately linearly with time at a rate of 0.45 s^{-1} (Fig. 6 *a*). In contrast, the amount of ^{14}C-label in the microtubules remained constant during this period, indicating that the microtubules were at polymer mass steady state (Fig. 6 *b*). During the chase period, some ^{3}H-label was initially lost from microtubules in a rapid burst, after which essen-

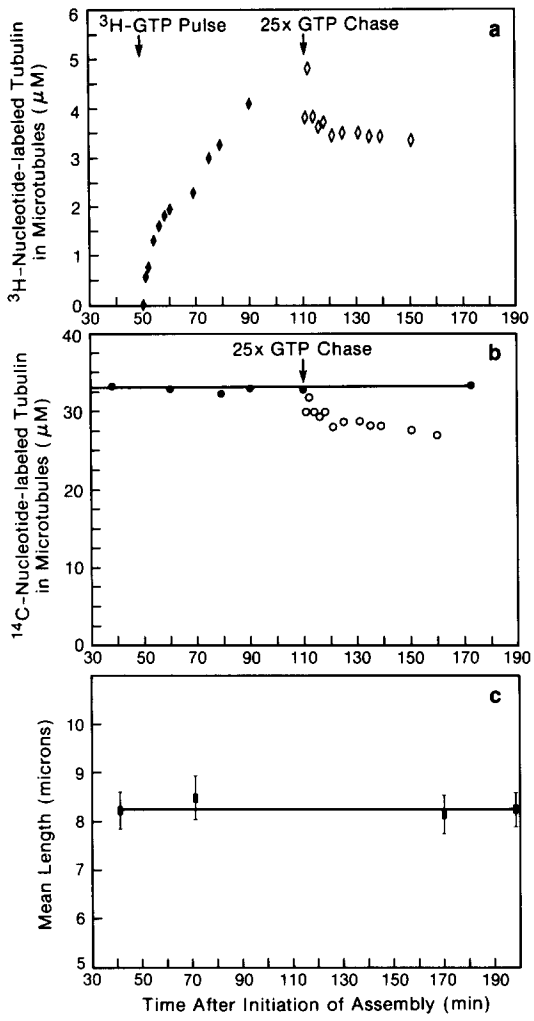

Figure 6. The dynamics of radionucleotide exchange with steady-state MAP-rich microtubules. Microtubules were assembled undisturbed from MAP-rich tubulin solutions (total protein concentration 4.12 mg/ml) at 30°C in MEM, 0.2 mM [^{14}C]GTP (10.7 Ci/mole) with a GTP-regenerating system. After 50 min (30 min at steady state), the microtubules were pulsed with [^{3}H]GTP (137 Ci/mole) for 40 min, followed by a 25-fold chase with unlabeled GTP for 40 min more. Microtubule aliquots (40 μl) were removed at intervals and processed by the filter assay procedure (Materials and Methods) to determine the amount of ^{3}H-nucleotide (*a*) and ^{14}C-nucleotide (*b*) in the microtubules. Closed symbols, pulse; open symbols, chase. (*c*) The lengths of the microtubules were determined after fixation in glutaraldehyde-MEM (print magnification of 6,500×, >280 microtubules per time sample, error bars ±1 SEM).

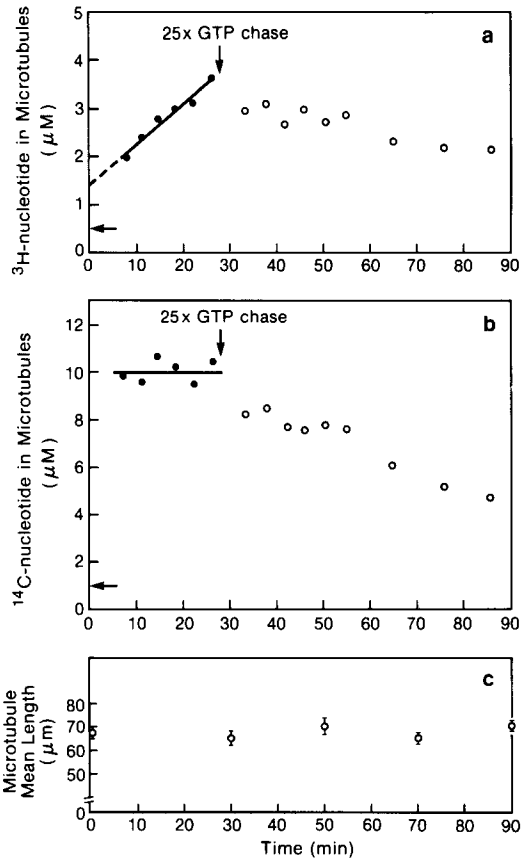

Figure 7. The dynamics of radionucleotide exchange with steady-state MAP-depleted microtubules. Microtubules were assembled undisturbed from MAP-depleted tubulin solutions (total protein concentration, 5.5 mg/ml) at 37°C in Pipes polymerization buffer containing 0.1 mM [^{14}C]GTP (6.36 Ci/mole). After 30 min at steady state (66 min after assembly initiation) the microtubules were pulsed with a trace of [^{3}H]GTP (38.2 Ci/mole) for 27 min, followed by a 25-fold chase with unlabeled GTP for a further 60 min. Microtubule aliquots (75 μl) were sedimented to determine the amount of ^{3}H-nucleotide (*a*) and ^{14}C-nucleotide (*b*) in the microtubules. Closed symbols, pulse; open symbols, chase. Horizontal arrows indicate the background level of (unincorporated) radiolabeled GTP (see Materials and Methods). All data points represent the mean values of triplicate samples. (*c*) The mean length of the microtubules were determined after fixation (final print magnification, 570×, >200 microtubules measured per time sample, error bars ±1 SEM).

tially no significant loss of label occurred (Fig. 6 *a*). The amount of ^{3}H-label lost during the loss burst (~1.4 μM) was approximately equal to the amount incorporated during the pulse uptake burst (~1.8 μM).

In contrast to the kinetics of ^{3}H-label loss, the ^{14}C-nucleotide was lost from the microtubules with biphasic kinetics (Fig. 6 *b*). There was an initially rapid loss of ^{14}C-nucleotide, followed by a phase in which the ^{14}C-label loss occurred linearly with time and at a rate (0.40 s^{-1}) approximately equal to the rate of [^{3}H]GTP uptake during the linear phase of the pulse. Again, the size of the burst of ^{14}C-label loss (2.5 μM) was approximately equal to that of the burst of ^{3}H-label loss or uptake (cf. Fig. 6, *a* and *b*). Throughout the entire pulse-chase period the microtubules were at polymer mass steady state (Fig. 6 *b*) and neither the mean length (Fig. 6 *c*) nor the length distribution (not shown) of the microtubules changed. These data, together with the kinetics of radiolabel exchange after the burst periods, are consistent with the steady-state microtubules undergoing treadmilling (see Discussion).

We also investigated the kinetics of radiolabeled subunit exchange with MAP-depleted microtubules with stable length distributions at polymer mass steady state. The experiments were performed as for MAP-rich microtubules, except that polymerization in [^{14}C]GTP was initiated using microtubule seeds which had been assembled previously

from tubulin solutions containing [^{14}C]GTP at the same specific activity as used in the experiment (Materials and Methods). A typical experiment is shown in Fig. 7.

After addition of the [^{3}H]GTP pulse, radiolabel incorporation into the microtubules proceeded with approximately linear kinetics, equivalent to a rate of 16.1 s^{-1} (Fig. 7 *a*). A burst of radiolabel uptake could not be directly observed because the airfuge sampling method used with MAP-depleted microtubules did not permit a large enough number of samples to be taken at very early times after addition of the [^{3}H]GTP. However, the presence of a burst of radiolabel incorporation can be inferred and its magnitude estimated from the linear regression line drawn through the experimental data points, which extrapolates to a point on the ordinate equivalent to ~1.4 μM ^{3}H-nucleotide. Subtracting the background of 0.5 μM, one calculates that a burst of radiolabel uptake into the microtubules equal to ~0.9 μM guanine nucleotide occurred within the first 7.5 min. The ^{14}C-nucleotide associated with the microtubules remained approximately constant during the pulse period, indicating the microtubules were at mass steady state (Fig. 7 *b*).

During the chase with excess unlabeled GTP, both ^{3}H- and ^{14}C-nucleotides were lost from the microtubules, in contrast to the situation with MAP-rich microtubules. However, the amount of ^{14}C-nucleotide lost during a 60-min chase (5.8 μM, Fig. 7 *b*) was nearly fourfold greater than the amount of ^{3}H-nucleotide lost during the same period (1.5 μM, Fig. 7 *a*). Furthermore, at 28 min into the chase, a period equal in length to the [^{3}H]GTP pulse time, only 27% of the ^{3}H-nucleotide was lost from the microtubules. This suggests that a diffusional exchange mechanism alone cannot account for the label loss. If it were the sole mechanism, the amount of ^{3}H-label lost would have been more than twofold greater than the amount actually lost (~59%, reference 40).

A loss burst of the two radionucleotides from the microtubules during the chase was not measured directly, but again this could be inferred by reasoning similar to that given above for a burst of incorporation. Values of 0.8 μM (^{3}H-label) and 0.7 μM (^{14}C-label) were calculated and are in close agreement with the size of the burst incorporation of ^{3}H-nucleotide. Throughout the pulse and chase periods the mean length (Fig. 7 *c*) and length distribution (not shown) of the microtubules remained constant.

Discussion

The Length Dynamics of MAP-rich and MAP-depleted Microtubules

The foregoing results demonstrate that in both unperturbed MAP-rich and MAP-depleted microtubule suspensions at steady-state, length redistributions were relatively small and occurred for only a short time after polymer mass steady state was attained (Tables I and II) or were not detectable (Figs. 1 and 5). Shearing the microtubules transiently increased the extent to which the length redistributions occurred, but again the microtubules relaxed to a state in which changes in the polymer length distributions were not detectable (Figs. 2, 3, and 5). MAP-rich and MAP-depleted microtubules differed in the extent to which the length distribution changes occurred. For MAP-rich microtubules, shearing or dilution induced mean length increases on the order of only 1 μm (Figs. 2–4). In contrast, the mean length of unperturbed MAP-depleted microtubules could increase by several micrometers at polymer mass steady state (Table II), and increases of 40–60 μm occurred in sheared preparations (Fig. 5; reference 30).

The differences between MAP-rich and MAP-depleted microtubules in the extent of the steady-state length redistributions were not due to temperature or buffer differences. We have examined the length redistributions of MAP-rich microtubules at 37°C in the Pipes polymerization buffer used for MAP-depleted microtubules and found the extent of the length redistribution to be essentially the same as in MEM at 30°C (data not shown). The results obtained with the MAP-rich microtubules were consistent with previous reports from this laboratory, in which no steady-state changes in the mean length of unperturbed MAP-rich microtubules were observed (38, 39).

The results described here are inconsistent with the conclusion of Kristofferson et al. (25) that unperturbed MAP-depleted microtubules at steady state in glycerol-free buffer do not achieve stable length distributions, but undergo substantial mean length increases. This conclusion appears to have been based on limited data (see Table III of reference 25).

The mechanistic basis for the length redistributions is unknown, although three models have been suggested. Job et al. (19) proposed that populations of steady-state MAP-depleted microtubules are composed of two subpopulations; one without MAPs and highly unstable, the other with MAPs and relatively stable. Upon dilution, the MAP-free microtubules rapidly lose subunits, which grow back onto the MAP-containing microtubules. This explanation does not appear to account for the experimental data for several reasons. First, if tubulin subunits added to the ends of MAP-containing microtubules, the ends of these microtubules would become MAP-free and would be indistinguishable from the ends of totally MAP-free microtubules. Very little length change should then occur. It is difficult to visualize how this mechanism could produce length changes of 40–60 μm (Fig. 5; reference 30), during which time 60–90% of the microtubules initially present disassemble completely. This model also does not explain why microtubules assembled undisturbed to polymer mass steady state should undergo length changes at all (e.g., Tables I and II). Horio and Hotani (16) have further observed visually that the ends of individual microtubules can frequently alternate between an elongating phase and a shrinking phase. These "excursions" can be several micrometers in length and also are not accounted for by the model of Job et al. (19). Finally, Kirschner and co-workers observed dynamic instability in microtubule suspensions in which MAPs could not be detected (25).

Recently, Murphy and co-workers (34) observed that steady-state microtubules at high number concentration can undergo endwise annealing, behavior which is enhanced by shearing, and they suggested that annealing might account for the steady-state mean length increase reported by Mitchison and Kirschner. However, with unperturbed microtubules at steady state, significant changes in the number concentration did not occur either with MAP-rich or MAP-depleted microtubules (Figs. 1 and 5; Tables I and II). Under these conditions, therefore, significant microtubule annealing did not occur. Microtubule annealing also does not appear to ac-

count for a significant proportion of the length redistributions observed with sheared or diluted microtubules. The length increase observed in MAP-rich microtubule suspensions after mild dilution could be entirely accounted for by tubulin subunit addition to the microtubules (Fig. 4 *b*). Kristofferson et al. (25), using biotinylated tubulin, also found little evidence for microtubule annealing with MAP-depleted microtubules under conditions similar to those used in this study. Further, the concentrations of microtubule ends employed in this study and in the work of Kristofferson et al. (10^{-11}–10^{-9} M) were at least an order of magnitude smaller than those employed by Murphy and co-workers ($\sim 6 \times 10^{-8}$ M), and would not favor the annealing reaction.

The third mechanism that has been proposed for the dynamic length changes of steady-state microtubules is based on the GTP "cap" hypothesis (6). Mitchison and Kirschner (30) suggested that the great majority of ends of steady-state microtubules are capped by GTP-tubulin dimers which stabilize them. Microtubules that lose their GTP caps, exposing the underlying GDP-dimers, depolymerize very rapidly. The subunits lost from the uncapped microtubules would regrow onto the remaining capped microtubules. These investigators further argued that both the loss and regain of a GTP cap must occur only rarely. Since the dissociation rate of GDP-tubulin from uncapped microtubule ends is in excess of 550 s^{-1} (30), loss of a cap without significant probability of cap regain would effectively result in complete disassembly of a microtubule. This could account for the continuous increase in the mean length and decrease in the number concentration of steady-state microtubule populations.

The GTP cap mechanism seems the most reasonable, and, with some modification, could account for all of our experimental observations. The enhancement of steady-state length redistributions produced by shearing or diluting the microtubules would be expected by the GTP cap model, since both treatments would increase the proportion of uncapped microtubules as well as generate shorter ones. Consequently, many more microtubules would depolymerize completely when compared with undisturbed microtubules, thus resulting in relatively large increases in the mean lengths of the microtubules as well as prominent changes in the length distributions (Figs. 2–5).

Our results suggest that a significant modification of the GTP cap model, as proposed by Mitchison and Kirschner (30), is necessary. Although length increases did occur initially in both MAP-rich and MAP-depleted microtubules, and under both perturbed and unperturbed conditions, our data indicate that microtubules rapidly attain a stable state in which further length changes are not detectable (Figs. 2–5, Tables I and II). These data suggest that if GTP cap dynamics are the basis of the length changes, a mechanism must exist for rapid recapping of microtubule ends that have lost caps (see also reference 4).

The probability of an uncapped microtubule completely depolymerizing would then be a function of the length of time required to recap a microtubule end, and the dissociation rate of GDP-dimers from that end, with shorter microtubules having a greater chance of disassembling completely than longer ones. The variation in stability of unperturbed microtubule distributions that we have seen during early times at steady state may thus be related to the proportion of short microtubules in the sample. In microtubule samples with few short microtubules, length changes would be undetectable (Fig. 1, steady-state mean length ~18 μm). More prominent length changes would be expected, however, in unperturbed microtubule samples with a large proportion of short microtubules, in some cases resulting in mean length increases comparable with those of sheared microtubules (cf. Table I, steady-state mean length 5–7 μm). With time, as the shortest microtubules disappear from the population, the remaining microtubules would have a low, but non-zero, probability of depolymerizing completely. Changes in the length distribution would thus diminish with time at steady state (Figs. 2–5, Tables I and II) as the microtubule population relaxed toward thermodynamic length equilibrium.

The process whereby a GTP cap could reform is not known, but in principle at least two mechanisms are possible. Either a sufficient number of GTP-tubulin subunits add to a GDP end, or GTP free in solution exchanges with GDP complexed with tubulin at a microtubule end. The first mechanism seems unlikely, since the rate of subunit loss from uncapped MAP-depleted microtubules is in excess of 550 s^{-1} (30), while the rate of GTP subunit addition to microtubules under steady-state conditions is only 15–30 s^{-1} (Fig. 8; reference 8). A qualitatively similar argument can also be made for MAP-rich microtubules. Evaluation of the second recapping mechanism is currently not possible, since the rate of exchange of free GTP with GDP subunits at microtubule ends, if it occurs, remains to be measured.

Although stable microtubule length distributions were observed (e.g., Figs. 1–5), it is unlikely that the apparent stability represents the final, true thermodynamic length equilibrium. For MAP-depleted microtubules with a mean length of 80 μm at true equilibrium, and assuming a steady-state macroscopic dissociation rate of 550 s^{-1}, a gross overestimate (30), it would take several months to reach true length equilibrium. This conclusion is supported by the observation that the mean length of sheared microtubules increased beyond that of unsheared and apparently stable microtubules, even though both microtubule populations were assembled from identical tubulin solutions (Fig. 5). For experimental purposes, however, the microtubule length distributions have effectively stabilized and further length increases would occur so slowly as to be undetectable.

Evidence for the Coexistence of Microtubule Length Changes and Treadmilling

It has been suggested (25, 30) that the exchange of tubulin subunits that accompanies steady-state microtubule length redistributions might account for the kinetics of radiolabeled GTP-tubulin exchange with microtubules at steady state, which we have interpreted as treadmilling (10, 11, 27). This suggestion is too simple to account for the data, however. The kinetics of radiolabeled GTP exchange with microtubules are complicated, and indicate that more than one reaction is involved.

For example, it is clear that tubulin subunit exchange during microtubule length redistributions, induced by dilution of MAP-rich microtubules, resulted in the initial incorporation of radiolabeled GTP into microtubules at a relatively rapid rate (Fig. 4 *a*). With time, however, the microtubule length distribution stabilized, yet label uptake by the microtubules continued at a slower and approximately linear rate.

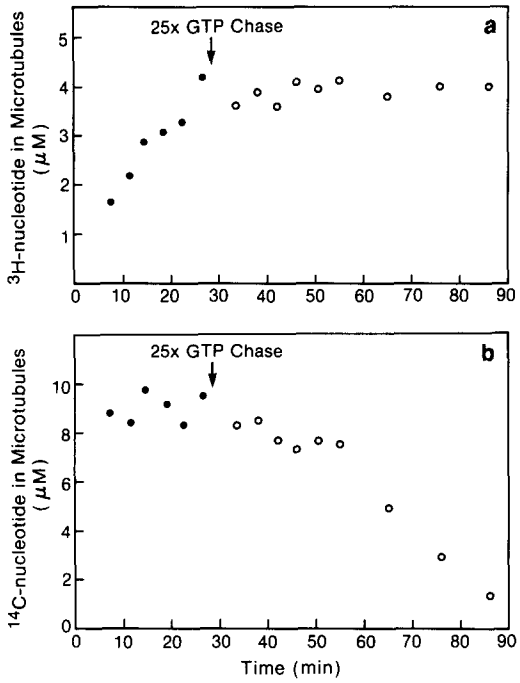

Figure 8. The data shown in Fig. 7 were corrected for ^{3}H-nucleotide (*a*) and unlabeled nucleotide (*b*) treadmilling completely through some microtubules. The corrections were calculated from the initial rate of [^{3}H]GTP uptake (16.1 s^{-1}), determined during the pulse period by linear regression analysis of the data in Fig. 7 *a*, and from the initial microtubule length distribution at the start of the pulse. Closed symbols, pulse; open symbols, chase. The length distribution did not significantly change during the pulse-chase period of the experiment.

The slow, linear phase of incorporation in the absence of microtubule length changes is consistent only with the treadmilling reaction (e.g., 22, 38, 39). The data indicate that when microtubule length increases are occurring, tubulin subunit addition due to net microtubule growth can predominate and overwhelm that due to the treadmilling reaction. When the length distribution stabilizes, tubulin addition due to the treadmilling reaction is observed.

Evidence for the coexistence of two types of microtubule behavior is also apparent from the results of isotope exchange experiments at steady state when no net length changes occur. Incorporation of [^{3}H]GTP occurred with biphasic kinetics (Figs. 6 and 7). An initial rapid burst of label uptake was followed by a slower, linear rate of incorporation. The initial burst is directly measurable with MAP-rich microtubules (Fig. 6 *a*), but not with MAP-depleted microtubules because of methodological limitations (see Results). However, the occurrence of a burst in MAP-depleted preparations can be inferred because the linear phase of label incorporation extrapolated to levels higher than background at time zero (Fig. 7 *a*). Similarly, a rapid burst of ^{3}H- and ^{14}C-nucleotide loss from the microtubules occurred immediately after chases with excess unlabeled GTP (Figs. 6 and 7). The sizes of the chase bursts were essentially the same, even though the ^{14}C-nucleotide was distributed throughout the microtubules, whereas the ^{3}H-nucleotide was confined predominantly to relatively short regions at microtubule assembly ends, with some label possibly at the opposite microtubule ends (e.g., 22, 40). The similarity of the chase burst sizes indicates that this loss occurs at the microtubule ends.

The burst reactions may reflect rapid steady-state transitions between shrinking and growing phases at microtubule ends (16) that do not change the overall microtubule length distributions. From the fraction of ^{14}C-nucleotide lost during the chase burst, and from the mean length of the microtubule population, we calculated that the amount of label lost was equivalent to a microtubule length of ~0.6 μm for MAP-rich microtubules (Fig. 6 *b*) and 4.5 μm for MAP-depleted microtubules (Fig. 7 *b*). This latter value is in close agreement with the size of the microtubule and excursions observed by Horio and Hotani for MAP-depleted microtubules (~1–5 μm) (16) and suggests that end excursions may account, perhaps in part, for the burst phase of nucleotide exchange with steady-state microtubules. However, we cannot exclude the possibility that part or all of the burst reactions represent exchange of GTP in solution with nucleotide exchangeably bound at microtubule ends.

The slow, linear phases of label uptake and loss by steady-state microtubules are consistent only with the treadmilling reaction. The linear rate of incorporation of a [^{3}H]GTP pulse occurred at essentially the same rate as the linear rate of loss of ^{14}C-nucleotide from the microtubules during a chase with unlabeled GTP (Figs. 6 and 7). For MAP-rich microtubules, the steady-state flux rate was 0.40–0.45 s^{-1} (~1 μm/h), in close agreement with values previously reported for this microtubule preparation (e.g., 38, 39). In contrast, a much faster flux rate was observed for MAP-depleted microtubules (24.6 s^{-1}, 52.5 μm/h, Fig. 8, discussed below), a value similar to that reported by Cote and Borisy (8).

The degree of retention of the ^{3}H-label during a chase with unlabeled GTP further supports the treadmilling interpretation. In MAP-rich microtubules, after the initial burst of label loss, essentially all the remaining ^{3}H-nucleotide was retained in the microtubules for the duration of the chase (Fig. 6 *a*). This is consistent with the treadmilling mechanism, and also demonstrates that the kinetics of radionucleotide incorporation into microtubules during the slow, linear phase do not result from an equilibrium exchange mechanism (40). If equilibrium exchange had been the sole mechanism, ~59% of the ^{3}H-label incorporated during the pulse would have been lost during the chase during a time interval equal in duration to the pulse period (28 min, Fig. 6, see references 22, 40).

Analysis of isotope exchange experiments using MAP-depleted microtubules is more complicated, probably due to the extremely rapid steady-state flux rate. During the chase period with unlabeled GTP, some loss of the ^{3}H-label did occur (Fig. 7 *a*). Two observations suggest that the loss was due to the label treadmilling completely through the shorter microtubules. First, the amount of ^{3}H-labeled dimers lost at the end of the 60-min chase (~1.5 μM) was only approximately one-fourth the amount of ^{14}C-labeled subunits lost (5.8 μM) during the same period (Fig. 7, *a* and *b*), and >50% of the ^{3}H-labeled subunits remained in the microtubules. If incorporation and subsequent loss of the ^{3}H-label was due to an equilibrium exchange mechanism rather than to a rapid flux rate, all of the ^{3}H-nucleotide should have been lost from the microtubules to be consistent with the amount of ^{14}C-nucleotide lost. Secondly, 28 min into the chase (the

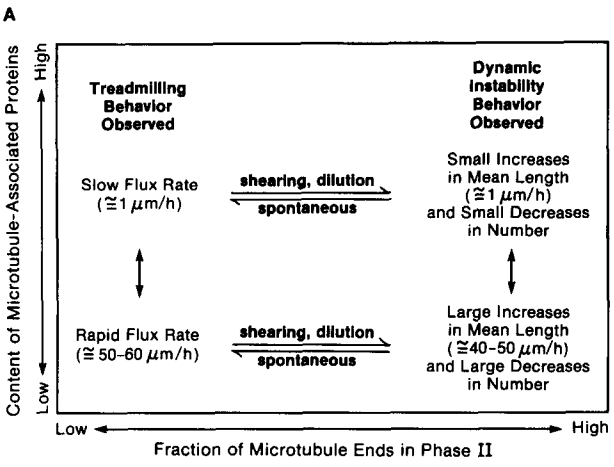

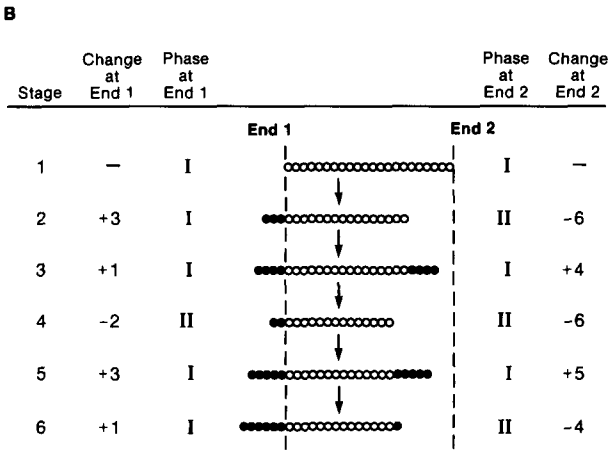

Figure 9. Microtubule Phase Dynamics. (*A*) Population dynamics. The observed macroscopic behaviors of microtubule populations are shown in relation to the MAP content and the fraction of microtubule ends in phase II. Treadmilling is the balanced addition of tubulin at one microtubule end (growth) and loss at the opposite end (shortening) (27). Dynamic instability is the reduction in microtubule numbers due to the complete depolymerization of some microtubules and the consequent increase in mean length of the remaining microtubules (29, 30). Phase transitions could be due mechanistically to gain (phase I) and loss (phase II) of short regions of GTP-tubulin caps at microtubule ends, but other mechanistic explanations exist. Transitions between phase II and phase I (cap regain) occur rapidly and independently at each end, and phase I ends have a significantly lower critical concentration than phase II ends. When unperturbed, most microtubule ends are in phase I at any instant and length distributions are stable unless a high proportion of short microtubules exists. Shearing or dilution induces a transient increase in the proportion of ends in phase II and/or creates an increase in the proportion of short microtubules. Values in parentheses are those obtained in the experiments described in this investigation. (*B*) Possible changes at the ends of a single microtubule. Some successive, but nonconsecutive stages are shown for a single microtubule. Open circles represent the subunits present in the microtubule at stage 1. Solid subunits have been added during subsequent stages. At stage 1, both microtubule ends are shown in phase I (growth phase). At stage 2, end 2 has transitioned to phase II and is depolymerizing (lost six subunits). End 1 remains in phase I and is growing (gained three subunits). At stage 3, end 2 has transitioned to phase I (four subunits added), while end 1 has remained in phase I (one additional subunit added). Subsequent possible stages are shown in like manner. Phase changes at the ends are occurring simultaneously with treadmilling. The kinetically slower end (end 1) is depicted as the net growing end, while the kinetically rapid end (end 2) is the net shortening end (see 39).

length of the pulse period), only 27% of the ^{3}H-nucleotide was lost from the microtubules. As discussed above for MAP-rich microtubules, this implies that an equilibrium exchange mechanism cannot account for the slower phase of labeled subunit exchange with MAP-depleted microtubules.

The amount of ^{3}H-label loss expected to occur by treadmilling during a chase was calculated from the microtubule length distribution, assuming that the rate of [^{3}H]GTP pulse incorporation into the MAP-depleted microtubules (16.1 s^{-1} or 34.4 μm/h, Fig. 7 *a*) was due to treadmilling. Essentially all of the ^{3}H-label lost during the chase could be accounted for on this basis (Fig. 8 *a*). Correcting both uptake and loss data for label treadmilling completely through short microtubules, one obtains a corrected rate of ^{3}H-label uptake of 24.6 s^{-1} (52.5 μm h^{-1}) and a corrected rate of ^{14}C-label loss of 28.5 s^{-1} (60.8 μm h^{-1}) (Fig. 8, *a* and *b*).

Phase Dynamics at Microtubule Ends

The results described in this paper demonstrate that exchange of tubulin at microtubule ends can occur by at least two pathways, described as treadmilling (23, 27, 28) and dynamic instability (30), at polymer mass steady state (diagrammed in Fig. 9 *a*). As indicated, the type of dynamic behavior that is observed is determined by the experimental protocols. Significant differences in experimental protocols may account for the apparently inconsistent results of previous investigations (11, 27, 29, 30, 39).

The molecular mechanisms underlying the diverse microtubule behaviors is presently unknown, but may be due to phase transitions at microtubule ends (7). As indicated, one mechanistic basis for the existence of two phases at microtubule ends could be the presence (phase I) or absence (phase II) of short regions of GTP-tubulin (i.e., GTP caps; 5, 6). If microtubule ends that lose the GTP cap are rapidly recapped, most microtubules would only partially depolymerize; rarely would a microtubule disassemble completely. In microtubule suspensions at polymer mass steady state, the rapid recapping of uncapped microtubule ends would lead to length distributions that changed so slowly with time as to appear stable (Figs. 1, 2, and 5). Under these conditions, although both ends of microtubules may continually shorten and regrow (16), the time-averaged result is a net addition of tubulin at one microtubule end and an equivalent net loss from the opposite microtubule end (Fig. 9 *b*). This would give rise to the flux of subunits through the microtubules, inferred from the kinetics of radiolabeled nucleotide exchange with steady-state microtubules (Figs. 6–8; references 11, 27).

In contrast, shearing microtubules or diluting microtubule suspensions would increase the number of short microtubules and/or the proportion of microtubule ends in phase II (uncapped), would would result in enhanced depolymerization (6, 12). If a significant number of microtubules are sufficiently short that they depolymerize completely before phase I can be reestablished (cap regain), an increase in the mean length of the microtubule population will occur (Figs. 2–5 and 9 *a*; reference 30) due to regrowth of the tubulin subunits lost from these microtubules onto the phase I ends

of the surviving microtubules. With time, however, the system would relax to a steady state in which the microtubule ends continually shorten and regrow without causing a net change in the length distribution, and, simultaneously, there would be net growth at one microtubule end and equivalent net shortening at the other end.

Kirschner and Mitchison have emphasized the importance of microtubule depolymerization in mitotic spindle formation and cell morphogenesis and have suggested that dynamic instability may play a fundamental role in the depolymerization of microtubules in cells (24). However, the stability of the microtubule length distributions (Figs. 1, 2, and 5) and the data of Horio and Hotani (16) indicate that microtubules in vitro "prefer" to remain in the polymerized (GTP-capped) state under the conditions employed. If this is also true of microtubules in cells, then there must be a mechanism in cells for actively depolymerizing microtubules, perhaps by removing or by suppressing reformation of GTP caps.

We thank Dr. Michael Caplow and Dr. Roger Leslie for lively and helpful discussions and suggestions.

This work was supported by United States Public Health Service grant NS13560 (L. Wilson) and GM26732 (K. W. Farrell).

Received for publication 28 August 1986, and in revised form 8 December 1986.

References

1. Asnes, C. F., and L. Wilson. 1979. Isolation of bovine brain microtubule protein without glycerol: polymerization kinetics change during purification cycles. *Anal. Biochem.* 98:64–73.
2. Bergen, L. G., and G. G. Borisy. 1980. Head-to-tail polymerization of microtubules in vitro. Electron microscope analysis of seeded assembly. *J. Cell Biol.* 84:141–150.
3. Bradford, M. M. 1976. A rapid and sensitive method for the quantitation of microgram quantities of protein utilizing the principle of protein-dye binding. *Anal. Biochem.* 72:248–254.
4. Caplow, M., J. Shanks, and B. P. Brylawski. 1985. Concerning the anomalous kinetic behavior of microtubules. *J. Biol. Chem.* 260:12675–12679.
5. Carlier, M.-F., and D. Pantaloni. 1981. Kinetic analysis of guanosine 5′-triphosphate hydrolysis associated with tubulin polymerization. *Biochemistry.* 20:1918–1924.
6. Carlier, M.-F., T. L. Hill, and Y.-D. Chen. 1984. Interference of GTP hydrolysis in the mechanism of microtubule assembly: an experimental study. *Proc. Natl. Acad. Sci. USA.* 82:771–775.
7. Chen, Y.-D., and T. L. Hill. 1985. Theoretical treatment of microtubules disappearing in solution. *Proc. Natl. Acad. Sci. USA.* 82:4127–4131.
8. Cote, R. H., and G. G. Borisy. 1981. Head to tail polymerization of microtubules in vitro. *J. Mol. Biol.* 150:577–602.
9. Dustin, P. 1984. Microtubules. Springer-Verlag, New York. 1–482.
10. Farrell, K. W., J. A. Kassis, and L. Wilson. 1979. Outer doublet tubulin reassembly: evidence for opposite end assembly-disassembly at steady state and a disassembly end equilibrium. *Biochemistry.* 12:2642–2647.
11. Farrell, K. W., and M. A. Jordan. 1982. A kinetic analysis of assembly-disassembly at opposite microtubule ends. *J. Biol. Chem.* 257:3131–3138.
12. Farrell, K. W., R. H. Himes, M. A. Jordan, and L. Wilson. 1983. On the nonlinear relationship between the initial rates of dilution-induced microtubule disassembly and the initial free subunit concentration. *J. Biol. Chem.* 258:14148–14156.
13. Farrell, K. W., and L. Wilson. 1984. Tubulin-colchicine complexes differentially poison opposite microtubule ends. *Biochemistry.* 23:3741–3748.
14. Gaskin, F., C. R. Cantor, and M. L. Shelanski. 1974. Turbidimetric studies of the in vitro assembly and disassembly of porcine neurotubules. *J. Mol. Biol.* 89:737–758.
15. Hill, T. L., and Y.-D. Chen. 1984. Phase changes at the end of a microtubule with a GTP cap. *Proc. Natl. Acad. Sci. USA.* 81:5772–5776.
16. Horio, T., and H. Hotani. 1986. Visualization of the dynamic instability of individual microtubules by dark-field microscopy. *Nature (Lond.).* 321:605–607.
17. Inoué, S., and H. Sato. 1967. Cell motility by labile association of molecules. *J. Gen. Physiol.* 50:259–292.
18. Inoué, S. 1964. Organization and function of the mitotic spindle. In Primitive Motile Systems in Cell Biology. R. D. Allen, editor. Academic Press, Inc., New York. 549–594.
19. Job, D., M. Pabion, and R. L. Margolis. 1985. Generation of microtubule stability subclasses by microtubule-associated proteins: implications for the microtubule "dynamic instability" model. *J. Cell Biol.* 101:1680–1689.
20. Johnson, K. A., and G. G. Borisy. 1977. Kinetic analysis of microtubule self-assembly in vitro. *J. Mol. Biol.* 117:1–31.
21. Johnson, K. A., and G. G. Borisy. 1979. Thermodynamic analysis of microtubule self-assembly in vitro. *J. Mol. Biol.* 133:199–216.
22. Jordan, M. A., and K. W. Farrell. 1983. Differential radiolabelling of opposite microtubule ends: methodology, equilibrium exchange-flux analysis, and drug poisoning. *Anal. Biochem.* 130:41–53.
23. Kirschner, M. 1980. Implications of treadmilling for the stability and polarity of actin and tubulin polymers in vivo. *J. Cell Biol.* 86:330–334.
24. Kirschner, M., and T. Mitchison. 1986. Beyond self-assembly: from microtubules to morphogenesis. *Cell.* 45:329–342.
25. Kristofferson, D., T. Mitchison, and M. Kirschner. 1986. Direct visualization of steady state microtubule dynamics. *J. Cell Biol.* 102:1007–1019.
26. MacNeal, R. K., B. C. Webb, and D. L. Purich. 1977. Neurotubule assembly at substoichiometric nucleotide levels using a GTP regenerating system. *Biochem. Biophys. Res. Commun.* 74:440–447.
27. Margolis, R. L., and L. Wilson. 1978. Opposite end assembly and disassembly of microtubules at steady state in vitro. *Cell.* 13:1–8.
28. Margolis, R. L., L. Wilson, and B. I. Kiefer. 1978. Mitotic mechanism based on intrinsic microtubule behaviour. *Nature (Lond.).* 272:450–452.
29. Mitchison, T., and M. Kirschner. 1984. Microtubule assembly nucleated by isolated centrosomes. *Nature (Lond.).* 312:232–237.
30. Mitchison, T., and M. Kirschner. 1984. Dynamic instability of microtubule growth. *Nature (Lond.).* 312:237–242.
31. Oosawa, F., and S. Asakura. 1975. Thermodynamics of the Polymerization of Protein. Academic Press, London. 1–204.
32. Roberts, K., and J. S. Hyams. 1979. Microtubules. Academic Press, Inc., New York. 1–595.
33. Rothwell, S. W., W. A. Grasser, and D. B. Murphy. 1985. Direct observation of microtubule treadmilling by electron microscopy. *J. Cell Biol.* 101:1637–1642.
34. Rothwell, S. W., W. A. Grasser, and D. B. Murphy. 1986. End-to-end annealing of microtubules in vitro. *J. Cell Biol.* 102:619–627.
35. Salmon, E. D. 1975. Spindle microtubules: thermodynamics of in vivo assembly and the role in chromosome movement. *Ann. N.Y. Acad. Sci.* 253:383–406.
36. Wegner, A. 1976. Head-to-tail polymerization of actin. *J. Mol. Biol.* 108:139–150.
37. Wilson, L., K. B. Snyder, W. C. Thompson, and R. L. Margolis. 1982. A rapid filtration assay for analysis of microtubule assembly, disassembly, and steady-state tubulin flux. *Methods in Cell Biol.* 24:159–169.
38. Wilson, L., H. P. Miller, K. W. Farrell, K. B. Snyder, W. C. Thompson, and D. L. Purich. 1985. Taxol stabilization of microtubules in vitro: dynamics of tubulin addition and loss at opposite microtubule ends. *Biochemistry.* 24:5254–5262.
39. Wilson, L., and K. W. Farrell. 1986. Kinetics and steady state dynamics of tubulin addition and loss at opposite microtubule ends: the mechanism of action of colchicine. *Ann. N.Y. Acad. Sci.* 466:690–708.
40. Zeeberg, B., R. Reid, and M. Caplow. 1980. Incorporation of radioactive tubulin into microtubules at steady state. Experimental and theoretical analyses of diffusional and directional flux. *J. Biol. Chem.* 255:9891–9899.